A Simple Real-Time Eye Tracking and Calibration Approach for Autostereoscopic 3D Displays

Chrisitan Bailer[1], José Henriques[1], Norbert Schmitz[1] and Didier Stricker[1]

[1]*Augmented Vision, German Research Center for Artificial Intelligence, Trippstadter Strasse 122, Kaiserslautern, Germany*
{Christian.Bailer, Jose.Henriques, Norbert.Schmitz, Didier.Stricker }@dfki.de

Abstract: In this paper a simple eye tracking and calibration approach for glasses-free stereoscopic 3D displays is presented that requires only one ordinary camera for tracking. The approach is designed for the use with parallax barrier based screens, but should with(out) limitations also be usable with other autostereoscopic screens. The robust eye tracking approach can easily be reimplemented and is based on well chosen search areas and parameters that were determined experimentally. Thanks to efficient eye position prediction delays can be eliminated that are normally a problem in realtime systems. The calibration approach allows us to calibrate the eye tracking camera to the 3D screen in a direct and simple way. Direct means that the calibration is realized pixel-wise and simple means that there is no need for a (complex) camera/screen model in contrast to many other calibration approaches. There is even no need to determine any camera parameter for calibration. The accuracy of the eye tracking approach and the eye position prediction is evaluated experimentally.

1 INTRODUCTION

Thanks to technological advances, glasses-based 3D displays are nowadays nearly as cheap as 2D displays, while they were still very expensive only a few years ago. This strongly promotes the distribution, but not necessary the acceptance, of 3D technology. Still 3D glasses are inconvenient to use. One first has to put them on before one can make use of the 3D effect. Furthermore, the glasses can be uncomfortable to wear especially for spectacle wearers, that have to wear two pairs of glasses at once. Moreover, the glasses darken the environment considerably which is a disadvantage for vision with indoor illumination. These disadvantages can be avoided by using glasses free 3D displays. They are still expensive – but similar to the price drop of glasses based 3D displays their price might drop significantly within the next few years.

Glasses free 3D displays can basically be divided into two classes: autostereoscopic displays and volumetric/holographic displays. Volumetric displays work by displaying the scene from many perspectives at once. This makes it besides the complexity of the display itself inapplicable for 3D movies, that were recorded from two perspectives only and hard for realtime rendering as extremely powerful hardware is necessary to render all perspectives at once.

Autostereoscopic displays on the other hand, only require two perspectives at a time like glasses based stereoscopic displays. To work this requires the user to either stay at a special spot in front of the display like with the Nintendo 3DS or eye position estimation (eye tracking) is required to determine at which coordinates in front of the screen the image for an eye is required.

In this work we present a parallax barrier based autostereoscopic 3D system with eye tracking. Our approach allows us to work with only one single camera for eye tracking. Usually eye tracking systems for 3D screens require either two cameras (Su et al., 2003; Perlin et al., 2001) or a depth camera (Li et al., 2012) as they need three dimensional eye positions. Also many eye tracking systems build on the red eye effect (Zhu et al., 2002) which requires pulsing infrared light that must be synchronized with the tracking camera. This requires a more expensive camera that has to have a good infrared sensibility (especially in bright rooms) and a higher framerate. Also, the setup is more complex. It is even more complex if the red eye effect is required in both cameras of a stereo camera setup (Perlin et al., 2001). Also such setups cannot deal well with fast eye movement especially if there are reflections e.g. on glasses.

Our tracking approach can be easily reimplemented as essential parts of the approach are based on
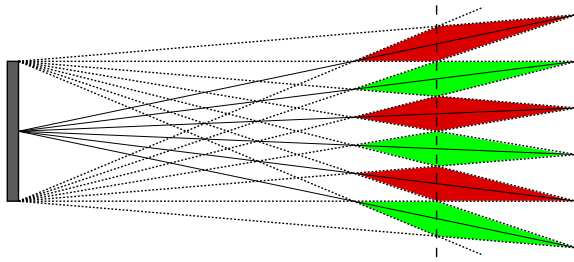
Figure 1: The (doted) rays from the left-most and right-most end of the screen are limiting the optimal viewing areas for both eyes. Green: Area where the image for the left eye is visible. Red: Area for the image of the right eye. The lines passing through the corners of the rhombuses meet at the middle of the screen. If the tracking camera is placed here there is no advantage anymore in determining the eye depth. See text for more details.
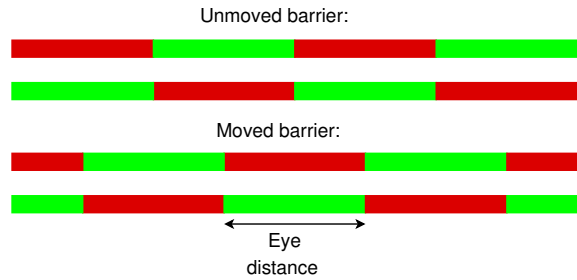

Figure 2: The stripes illustrate the colors on the dashed line in Figure 1. The width of a stripe is roughly the eye distance of a human. First row: original screen image. Second row: images for eyes are swapped. This creates different 3D areas. In theory every point is covered by these two states. In practice it will not work in the transit area if the eyes are not exactly in the depth of the dashed line in Figure 1. This can be solved by a movable barrier, which gives us in our case 4 different states.

established algorithms with publicly available source-code. Search areas (e.g. Figure 5) are chosen to work well for all tested persons plus some extra margin, while being strict enough to exclude outliers. The system can work under different lighting conditions (we tested it with sunlight as well as infrared light). A major benefit of the proposed setup is that the calibration approach is pixel-wise and thus does not require the determination of camera and screen parameters. Determining such parameters can be complicated especially if even two cameras must be calibrated to each other (Andiel et al., 2002).

The paper is structured as follows: In Section 2 we give an overview over our 3D system including the camera for tracking and the 3D screen. In Section 3 we are describing our approach of calibrating the tracking camera to the 3D screen. In Section 4 we describe the actual eye tracking system in detail. The eye tracking system includes eye tracking as well as eye detection elements. While we differ between the tracking and detection parts in Section 4 the term "eye tracking" is in other sections only used to refer to our whole eye tracking system. Finally, we evaluate and conclude our approach in Section 5 and 6, respectively.

2 THE 3D SYSTEM

In this section we describe our 3D system. The system consists of the following hardware parts: The 3D screen, the camera for eye tracking, a PC (Xeon E3 @3.4Ghz) running our software and infrared LEDS for optional night vision. The software consist of the eye tracking and calibration system. Our tracking camera is a common camera which operates at a resolution of 1216 x 866 pixels at 50 frames per second. Our 3D screen is based on the parallax barrier principle (see Fig. 2 in (Neil, 2005)) with multiple viewing zones (see Figure 1 and Fig. 3/4 in (Neil, 2005)). The barrier of our screen can be moved, so that we cannot only swap the image for the left and the right eye but have in common four possible states (Figure 2). For details on the technology concerning movable barriers see e.g. (Isono et al., 1993; Yi et al., 2008). The camera is placed at the intersection point of the rhombuses (Figure 1). Thereby we do not have to consider the depth (z value) for calibration and eye tracking as we can determine the best possible screen setting directly from pure 2D eye positions. Please note that although the intersection point in Figure 1 is in the center of the screen we can move the camera freely alongside the parallax barrier stripes (the dimension not visible in the figure). This allows us to place it on top of the screen. If the camera positioning opposed to the barrier is not accurate the size of the rhombuses is reduced slightly. In practice, a rough central placement is sufficient.

3 CALIBRATION

The goal of our calibration approach is to calibrate (assign) the pixel positions in the camera used for eye tracking directly to the appropriate states of the 3D screen. Assigning pixels directly allows us to calibrate the system without knowing all the relevant camera and screen parameters. This is a big advantage as the relevant screen parameters might even be vendor or model specific. To do so, we put the screen 2 meters away parallel to a wall (as this is the optimal distance of operation, dashed line in Figure 1). Then
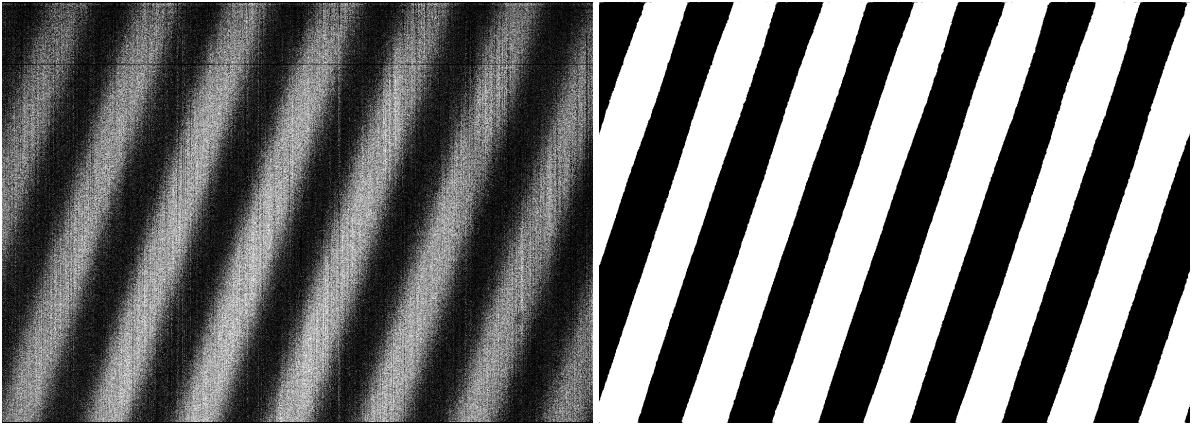
Figure 3: Left: One of the two input images with noise and image artifacts. Right: The resulting stripe pattern.

we render a black image for one eye and a white image for the other eye. In a dark room this creates a pattern like the one that can be seen in Figure 3 left. The pattern is too dark to be directly recordable by our camera. However, we can create the image by taking several images and averaging their brightness values to obtain the image I_L. Then we invert the screen illumination and take another averaged image I_R. Inverting the screen illumination means that we render a white image for the eye where we originally rendered a black image and vice versa. Then we compare I_R to I_L. If a pixel is brighter in I_R than in I_L we set this pixel to 1 in a new binary image I_B. Otherwise we set the pixel to 0. If we apply a median filter on I_B to remove single outliers we get the image visible in Figure 3 on the right side. As can be seen the stripes are nearly detected perfectly although the original images are noisy and contain artifacts. I_B could now be used to find camera parameters that lead to the determined pattern. However, this is unnecessary as it is more accurate and less effort to use I_B directly instead of approximating it with a model. In total we create 4 images I_B for the 4 states in Figure 2 which we call $I_B^1...I_B^4$. The first two are for the unmoved barrier and the last two for the moved barrier. Practically we do not save I_B^2 and I_B^4 as they are just the inverse of I_B^1 and I_B^3, respectively.

To determine the correct state for given eye positions from the eye tracker we first calculate the eye center position by averaging both eye positions. This makes sense as there is no advantage in treating them independently. In the unlikely case where our eye tracker (described below) only provides the position of one eye we take the head center (also provided by our eye tracker) for the x and the eye position as the y coordinate of the eye center position. To determine how well the eye center position fits to a state s we determine the distance of the eye center pixel to the

next white to black transit in the corresponding image I_B^s. The state where the transit is the closest from the eye center pixel is the state that is chosen.

Note that our direct calibration approach is also suited for displays with freely moving stripes even if it only provides two viewing spots at a time (See (Neil, 2005) Fig. 4b)) . We do not have to record a calibration pattern for every possible position or state as we can simply interpolate in between positions/states by the distances of the eye center position to the white black transit in the two best fitting calibration patterns.

4 THE EYE TRACKING SYSTEM

In this section we present our eye tracking system, which is outlined in Figure 4. In the first frame we perform eye detection to find the positions of the two eyes. If an eye is detected it is tracked in the next frame(s), but at the same time we also try to redetect it. This helps to get a more accurate position if the detection and tracking do not lead to the exactly same position. Furthermore, redetection helps us to update the appearance model of the tracker – however, we are not only considering the newly detected position for model update but also the previous one in our fusion approach. Thanks to redetection we can also still find the eye in frames where either tracking or detection fails. In the subsequent part of this section we will describe the individual parts of our approach in more detail. We also describe our prediction approach that predicts eye positions to eliminate delays.

4.1 Eye Detection

To be able to perform robust and fast eye detection we first use face detection to detect face candidates.
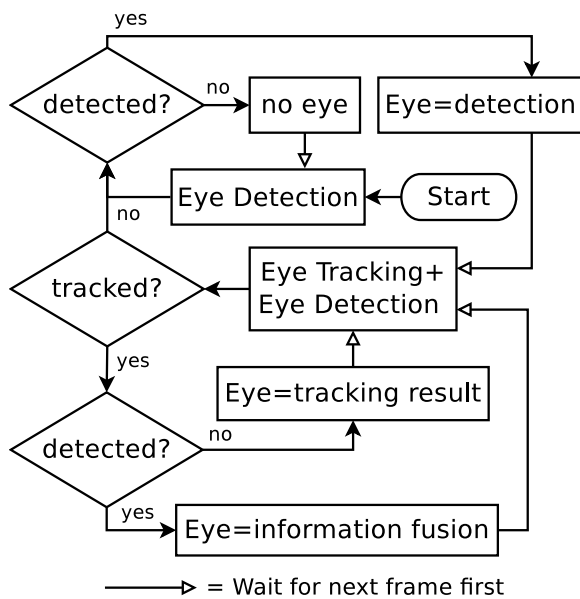
Figure 4: The eye tracking pipeline. "Eye=" means that the eye position is set from the stated value. "no eye" means that there is no eye detected in the frame.
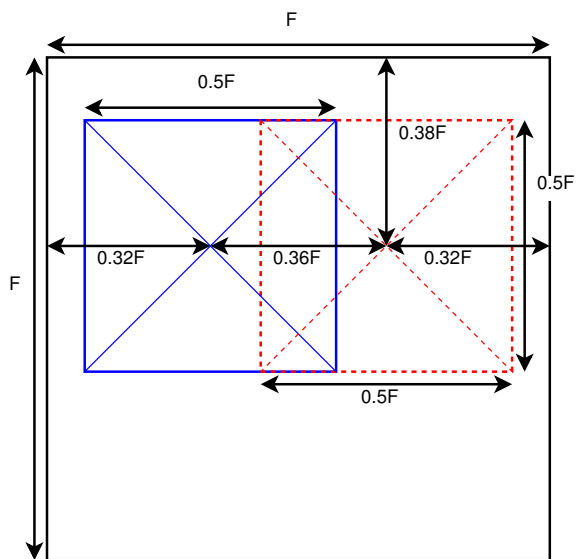

Figure 5: The search areas for the left eye (blue) and the right eye (dashed red) inside the area of a detected face. Values were determined carefully through experiments. Note that eyes are determined as areas i.e. the center of an eye position cannot be in the whole search area.

Face detection is performed on a scaled-down image to speed up detection. Scaling down the image usually does not drop the detection rate much as faces are much larger than eyes but clearly speeds up detection. Autostereoscopic displays usually have a limited working distance. Thus, we are searching the face only for face sizes that correspond to a distance in the range of operation $\pm$ 20%.

After one or multiple face candidates are found the eyes are searched in defined areas inside each face candidate (see Figure 5). If only one eye candidate is found inside the search area of each eye it is kept. Otherwise all of them are discarded. As this happens only seldom with our well chosen search areas we do not want to risk to choose the wrong one.

For eye and face detection we use Haar feature based cascade classifiers (Viola and Jones, 2001; Lienhart and Maydt, 2002). More precisely we are using the following pretrained classifiers that are publicly available in the OpenCV library[1]: "*haarcascade_frontalface_alt.xml*" for face detection and "haarcascade_mcs_lefteye.xml" and "haarcascade_mcs_righteye.xml" for the detection of left and right eye, respectively. The search size for eyes we set to be between 0.2 and 0.4 times the face size for the width and 2/3 of this value for the height.

In our tests we could not find a case where we found both eyes for false positive face candidates. Thus, we can robustly reject false positives by reject-

ing faces where we cannot find both eyes. If we find one eye we will reject the detected eye if we either detect another face with two eyes or if the tracked position contradicts with the detection. In case of two persons in the image we prefer the currently tracked person for a display like ours that supports 3D only for one person.

4.2 Eye Tracking

Eye tracking is performed by template matching. Template matching is fast and according to our tests in our case also more robust and accurate than many more advanced tracking methods. We found that one reason for this is the small size (in pixels) of our templates, which leads to poorer results with many feature based tracking methods. We also think that the appearance of eyes of having one central blob is advantageous for template trackers in case of appearance change. In frames where the eye is detected the eye template is created or updated from the image detail at the eye position. In frames where there is no detection it is not updated to avoid drifting. For robustness and speed, templates are only matched to a local image area where the eye is expected. The center of this area is at the eye position at the last frame plus the movement between the two last frames if available. If the matching score of the best position deceeds a threshold tracking fails without a valid position and the template is deleted.

As template matching function we are using Normalized Cross Correlation, which is robust to illumination changes. In OpenCV this can be easily utilized by using the *"matchTemplate"* function. To better be able to deal with appearance changes template matching is performed with a slightly Gaussian blurred template and image. Thanks to the blur, pixels do not have to fit perfectly and it rather improves matching accuracy than reducing it.

4.3 Information Fusion

Pixel-wise template matching is usually more accurate in position than object detectors that are based on coarse image features like Haar or HOG. We cannot directly benefit from the higher accuracy as the template is based on the detection. However, the tracker allows us to shift the detected eye position from one frame to the next. The shifted detection can then be directly compared to the detection in the next frame. This allows us to average the detected eye positions of the detector in different frames. Formally the eye position at a frame n, P_n is calculated as:

$$P_n = S_n + T_n \tag{1}$$

where T_n is the tracked position at frame n and S_n the shift correction calculated as:

$$S_n = \text{round}\left(\sum_{i=n-k+1}^{n} S_i^n / k\right) \tag{2}$$

$$S_n^n = D_n - T_n \tag{3}$$

$$S_n^{n+i} = S_n^{n+i-1} - S_{n+i} \tag{4}$$

D_n is the detected eye position and k the number of considered previous frames. A template with center P_n is used as new tracking template. In case that tracking fails the considered frames k must be reset to one. We define K= k_{max}.

4.4 Dealing with reflections on glasses

Reflections on glasses caused e.g. by sunlight or infrared illumination for tracking in the dark can distract our tracking and detection methods. The distraction can be reduced significantly by lowering the brightness value at brightness peaks caused by the reflections. To do so we determine for each pixel the average brightness of its local surrounding (We use the eye template size as the size of the local surrounding. See Section 5 for its size). If a pixel exceeds 3 times the average brightness or has the maximal representable brightness value it is considered to be part of the reflection and is set to the average brightness of

the local surrounding. By using integral images this approach can be implemented with very low runtime cost.

4.5 Temporal Prediction

A problem with realtime eye tracking for 3D displays is that there is a temporal delay i.e. the eye position is already outdated when calculated. Humans can recognize even a very short delay well. To prevent the delay we predict the eye position for a time where we do not yet have an image from the eye tracking camera. We test and compare two types of prediction, simple speed based prediction:

$$P_{n+i}^{(1)} = P_n + i(P_n - P_{n-1}) \tag{5}$$

and acceleration based prediction:

$$P_{n+i}^{(2)} = P_n + i(P_n - P_{n-1}) + 0.5i^2(P_n - 2P_{n-1} + P_{n-2}) \tag{6}$$

Our system has a delay of around 55 ms. 10 ms because the average eye position is in the middle of the exposure. The software delay from starting receiving a new image from the camera until a new state is send is around 25 ms (As steps for different frames can be performed in parallel we can still process more than 50 frames a second). We assume on average 15 ms delay for the time to the next display refresh plus the displays reaction time. Furthermore, we calculate 5 ms as extra delay e.g. for the time the graphics card actually needs to transmit an image. If makes no difference if the single eye positions are predicted before eye center calculation or if the eye center position is predicted directly.

5 EVALUATION

In this section we evaluate the accuracy of our eye tracking approach. For our tests we use a scale down factor of 2.5 for face detection. The template size for eye tracking we set to $0.2F \times 0.15F$, the template search area to $0.33F \times 0.25F$ and σ of the template blur to $0.02F$, with F being the detected face size. Tracking fails if the template matching error for the best position deceeds 0.8.

Our evaluation results can be seen in Table 1. We evaluated our tracking approach with 8 different persons and told them to move in different ways. Then we roughly categorized the different recordings according to their movement speed and accelerations. For "still" only slight movement and no big position change is allowed. However, people are not artificially trying to avoid movement completely. Slow

		Average location error in pixel									% frames with pixel error			
		Direct (P_n)			Speed Pred. $P^{(1)}_{n+3}$			Acc. Pred. $P^{(2)}_{n+3}$			Speed Pred. $P^{(1)}_{n+3}$			$P^{(2)}_{n+3}$
Per-son	Speed	K=1	K=2	K=3	K=1	K=2	K=3	K=1	K=2	K=3	$\geq$ 36	$\geq$ 24	$\geq$ 18	$\geq$ 18
1	still	1.26	1.26	**1.14**	2.68	1.60	**1.25**	6.43	2.54	**1.83**	0.0	0.0	0.0	0.0
3	still	2.53	**2.47**	2.67	3.67	2.66	**2.51**	7.97	4.05	**3.17**	0.0	0.0	0.0	0.0
5	still	0.33	0.28	**0.28**	1.53	1.17	**1.03**	5.24	**1.74**	1.94	0.0	0.0	0.0	0.0
1	slow	0.75	**0.67**	0.82	2.57	**2.25**	2.34	6.23	**4.31**	4.80	0.0	0.0	0.0	2.1
2	slow	1.84	2.10	**1.83**	3.60	3.03	**2.75**	7.74	**4.52**	4.86	0.0	0.0	0.0	3.0
3	slow	1.94	**1.78**	2.02	2.84	**2.80**	**2.80**	6.36	4.91	**4.37**	0.0	0.0	0.0	2.2
4	slow	0.97	**0.73**	0.81	2.78	**1.57**	1.94	7.65	**3.76**	4.12	0.0	0.0	0.0	0.0
5	slow	0.65	0.59	**0.59**	2.88	**2.42**	2.52	6.46	5.13	**4.38**	0.0	0.0	0.0	0.0
6	slow	**1.09**	1.14	1.13	2.42	2.03	**1.76**	5.09	3.58	**2.84**	0.0	0.0	0.0	0.0
2	middle	**1.63**	1.89	1.72	6.44	**5.60**	5.69	9.47	**6.61**	6.62	0.0	0.0	0.0	4.5
3	middle	1.64	**1.42**	1.69	7.12	6.44	**6.26**	11.27	7.94	**7.26**	0.0	0.0	1.6	9.8
4	middle	0.80	**0.64**	0.70	3.29	2.56	**2.43**	6.59	3.83	**3.38**	0.0	0.0	0.0	0.0
5	middle	0.92	0.88	**0.85**	3.91	3.65	**3.58**	7.48	6.45	**5.20**	0.0	0.0	0.0	8.6
6	middle	0.99	1.09	**0.99**	4.29	4.01	**3.71**	6.70	5.31	**4.89**	0.0	0.0	0.0	5.7
7	middle	1.39	**1.31**	1.34	5.18	4.46	**4.13**	10.16	6.94	**5.92**	0.0	0.0	0.0	3.6
8	still - fast	1.11	**0.89**	1.19	4.30	4.00	**3.99**	6.76	**4.78**	4.78	0.0	1.3	5.1	3.8
1	fast	0.90	**0.75**	0.97	5.03	**4.61**	5.53	8.25	**7.39**	7.80	0.0	5.5	15.0	11.0
2	fast	**2.47**	3.94	5.08	21.67	**20.29**	20.62	16.12	13.26	**12.85**	14.3	35.7	50.0	21.4
4	fast	1.38	**1.35**	1.76	11.91	11.79	**11.35**	9.08	10.12	**8.93**	0.0	4.2	25.0	12.5
7	very fast	**9.09**	9.33	11.22	**32.12**	33.12	33.99	64.54	**63.07**	67.21	23.5	41.2	52.9	64.7
∅	$\leq$ middle	1.24	**1.20**	1.24	3.72	3.14	**3.04**	7.35	4.77	**4.40**	0.0	0.1	0.4	2.7
∅	all	**1.68**	1.73	1.94	6.51	6.00	**6.00**	10.78	8.51	**8.36**	1.9	4.4	7.5	7.6

Table 1: Our evaluation results. We evaluated the location error for direct tracking and prediction of 3 frames (60ms). On the right we show the number of frames that exceed an error threshold. K is set to 2 for these threshold tests. Person 3,7 and 8 are wearing glasses. Please note that the overall average is strongly influenced by the few fast movement experiments, as there are great errors with fast movement. We show the overall average for completeness, but practically relevant is the average that excludes the unnaturally fast movement. The bold numbers show the best value of a K. See text for more details.

and middle corresponds to usual movement in front of the screen if the user wants to change his position or if he wants to test the 3D effect while moving. Fast and very fast are unnatural fast movements with very strong accelerations, that should only happen if one wants to find the limits of our system. Thus, we show fast movement only as completion as it is usually irrelevant for the practical application.

Figure 6: Circles: two inaccurate detections, one form the current frame and one shifted from the last frame. Doted circle: Average position of the two circles. Cross: ground truth. Only in the right example the doted circle is closer to the ground truth than the average distance of the two normal circles to the ground truth. As the position variations of the eye detector is mostly like on the left (one sided error) there is no big benefit for our information fusion approach in average pixel location error. However, the doted circle is less noisy in position than the original circles which supports prediction (see text).

The determined pixel error is the error of the eye center position (the average of both eye potions) compared to labeled ground truth, as the accuracy of the eye center position and not the accuracy of single eyes is relevant for our approach. As can be seen in Table 1 the pixel location error without prediction is for natural movement on average only 1.2 pixels (K=1), which are roughly 0.8 mm. Here, we cannot benefit much from information fusion on average location error.[2] Figure 6 shows a likely reason for it. However, if we use prediction the more stable and less noisy position is a real benefit and leads to clearly smaller pixel location errors especially for acceleration based prediction. Up to K=3 the average location error drops. For bigger K the shift error of several shifts in a row (errors are summing up) exceeds the benefit. Without prediction K=2 is already the limit. Although, acceleration based prediction benefits more from informa-

---

[2]But in the number of sequences where K=2 and K=3 is better than K=1 the difference is significant when excluding fast movement speed.

tion fusion it cannot compete with simple speed based prediction in accuracy. Thus, we practically use speed based prediction with K=3.

In our tests the measured stripe size was around 96 pixels. Thus, we can allow in the best case 48 in the average case 36 and in the worst case 24 pixels location error to be still in a correct screen state. In Table 1 we also measure the percentage of frames where the pixel error exceeds a limit (K=3 is used). In practice it is recommendable to stay below the theoretical values. Thus, we also tested for 18 pixels. As can be seen, even 18 pixels are no problem with speed based prediction for up to middle movement speed, while the limit is exceeded several times in different sequences with acceleration based prediction. In contrast, for fast movement speed, acceleration based prediction is often superior (also in accuracy). Practically, the user can (due to limit exceedances) see some flicker for fast movement, mainly when he abruptly starts or stops moving.

6 CONCLUSION

In this paper we presented an accurate calibration approach for or autostereoscopic 3D displays that does not require the knowledge of camera and screen parameters and is thus very universal and simple to apply. Furthermore, we presented an easily implementable but robust eye tracking system. In our evaluation we demonstrated its effectiveness. We showed that it mostly even works for very high movement speeds. Thanks to the temporal prediction and the information fusion that improves the prediction accuracy even a reaction delay of 60 ms is no real problem in our realtime autostereoscopic system. In future work we plan to expand our system to more complex autostereoscopic displays that can directly adapt to the users distance to the screen. We, for example, can determine the interocular distance with our eye tracker to calculate the rough viewing distance and calibration could e.g. be performed for two or more distances and in-between distances could be interpolated.

7 ACKNOWLEDGEMENT

REFERENCES

Andiel, M., Hentschke, S., Elle, T., and Fuchs, E. (2002). Eye tracking for autostereoscopic displays using web cams. In *Electronic Imaging 2002*, pages 200–206. International Society for Optics and Photonics.

Isono, H., Yasuda, M., and Sasazawa, H. (1993). Autostereoscopic 3-d display using lcd-generated parallax barrier. *Electronics and Communications in Japan (Part II: Electronics)*, 76(7):77–84.

Li, L., Xu, Y., and Konig, A. (2012). Robust depth camera based multi-user eye tracking for autostereoscopic displays. In *Systems, Signals and Devices (SSD), 2012 9th International Multi-Conference on*, pages 1–6. IEEE.

Lienhart, R. and Maydt, J. (2002). An extended set of haar-like features for rapid object detection. In *Image Processing. 2002. Proceedings. 2002 International Conference on*, volume 1, pages I–900. IEEE.

Neil, A. (2005). Autostereoscopic 3d displays. *Computer*, 8:32–36.

Perlin, K., Poultney, C., Kollin, J. S., Kristjansson, D. T., and Paxia, S. (2001). Recent advances in the nyu autostereoscopic display. In *Photonics West 2001-Electronic Imaging*, pages 196–203. International Society for Optics and Photonics.

Su, C.-H., Chen, Y.-S., Hung, Y.-P., Chen, C.-S., and Chen, J.-H. (2003). A real-time robust eye tracking system for autostereoscopic displays using stereo cameras. In *Robotics and Automation, 2003. Proceedings. ICRA'03. IEEE International Conference on*, volume 2, pages 1677–1681. IEEE.

Viola, P. and Jones, M. (2001). Rapid object detection using a boosted cascade of simple features. In *Computer Vision and Pattern Recognition, 2001. CVPR 2001. Proceedings of the 2001 IEEE Computer Society Conference on*, volume 1, pages I–511. IEEE.

Yi, S.-Y., Chae, H.-B., and Lee, S.-H. (2008). Moving parallax barrier design for eye-tracking autostereoscopic displays. In *3DTV Conference: The True Vision-Capture, Transmission and Display of 3D Video, 2008*, pages 165–168. IEEE.

Zhu, Z., Ji, Q., Fujimura, K., and Lee, K. (2002). Combining kalman filtering and mean shift for real time eye tracking under active ir illumination. In *Pattern Recognition, 2002. Proceedings. 16th International Conference on*, volume 4, pages 318–321 vol.4.